A Simple Simulation-derived Descriptor for the Deposition of Polymer-wrapped Carbon Nanotubes on Functionalized Substrates

Supporting Information

Zhizhang Shen,[1] Jonathan H. Dwyer,[1] Jian Sun,[2] Katherine R. Jinkins, [2] Michael S. Arnold, [2] Padma Gopalan[2], Reid C. Van Lehn[1]*

[1]Department of Chemical and Biological Engineering, University of Wisconsin-Madison, 1415 Engineering Drive, Madison, WI 53706, United States

[2]Department of Materials Science and Engineering, University of Wisconsin-Madison, 1509 University Avenue, Madison, WI 53706, United States

S1. Simulation Systems

The simulation system contained a single (6,5) semiconducting carbon nanotube (s-CNT) wrapped by three chains of poly[(9,9-dioctylfluorenyl-2,7-diyl)-*alt*-*co*-(6,6′-[2,2′- bipyridine])] (PFO-BPy), an amorphous silicon oxide slab grafted with a self-assembled monolayer, and toluene molecules. The s-CNT had a length of 6 nm and a diameter of ~0.75 nm. To match the length scale of the s-CNT, each chain of PFO-BPy was composed of five monomers in a *cis* configuration. Each PFO-BPy oligomer was initially wrapped around the s-CNT by rotating each monomer 30° around the polymerization axis with respect to the previous monomer; after equilibration for 20 ns in toluene the equilibrium wrapping angle was calculated to be 16.9° in good agreement with prior experimental measurements.[1] No restraints were added to the polymer and we did not observe substantial migration of the polymers on the s-CNT surface during any simulations. The amorphous silicon oxide surface had dimensions of ~12.10 × 12.43 × 3.0 nm^3. In order to make

comparisons consistent, we chose a surface coverage of 3.7 mole/nm^2 for all SAMs to match coverages used in prior simulations; this coverage led to general agreement between interfacial properties computed from the simulations and experimental measurements reported.[1]

S2. Molecular Dynamics Force Fields

The amorphous silica surface was modeled with the INTERFACE force field,[2] which has been shown to accurately predict interfacial properties (in water) for all types of silica and is compatible with common force fields for organic materials. All SAMs were described using AMBER-compatible force field parameters. The force field parameters were taken from the literature[3,4] for SAMs composed of only alkyl chains and from the General Amber Force Field (GAFF)[5] for other SAMs where the parameters were not found in the previously mentioned literature.[3,4] Atomic charges for atoms in SAMs were derived from quantum mechanical calculations at the HF/6-31G* level of theory using the RESP charge fitting method[6] and AmberTools18[7]. We modeled the s-CNT using a recently updated INTERFACE force field[8] which employs virtual π electrons to account for the π electron density and multipoles in graphitic layers. The force field parameters for PFO-BPy were also obtained from GAFF[5] with atomic changes derived from quantum mechanical calculations of a dimer of PFO-BPy at the HF/6-31G* level of theory using the RESP charge fitting method.[6] The combination of INTERFACE/GAFF parameters for the s-CNT and polymer wrapper was selected for compatibility with the INTERFACE/AMBER combination used for the SAM-grafted silica surface. Force field parameters and atomic charges for toluene were described by GAFF.[5]

S3. Potential of Mean Force (PMF) Calculations

To compute the free energy for s-CNT adsorption to SAM-grafted silica surfaces, we performed umbrella sampling and constructed PMFs from the umbrella histograms using the weighted histogram analysis method (WHAM[9]). The reaction coordinate for umbrella sampling was the distance along the *z*-axis between the center-of-mass of the s-CNT and that of the SAM-grafted silica slab (denoted as *z*). 20 windows separated by 0.1 nm were used in the umbrella sampling calculations. For each window, the distance was restrained to the target value using a harmonic potential with a spring constant of 5000 kcal mol^{-1} nm^{-2}. The angle between the s-CNT long axis and the *z*-axis of the simulation box was restrained to 90° using a harmonic potential with a spring constant of 5000 kcal mol^{-1} rad^{-2}. This restraint was added to prevent the s-CNT from tilting because tilting would be promoted for the short s-CNTs (~6 nm) studied computationally but less likely to affect adsorption for the longer s-CNTs (~100 nm) studied experimentally.

Initial configurations for umbrella sampling were generated using steered molecular dynamics (MD) in which a harmonic potential with a spring constant of 5000 kcal mol^{-1} nm^{-2} was applied to pull the s-CNT along the reaction coordinate. In order to test whether hysteresis would affect the PMFs, initial frames for umbrella sampling were taken from both descending (*i.e.*, steered MD simulations in which the value of *z* was decreased) and ascending (*i.e.*, steered MD simulations in which the value of *z* was increased) simulations. The initial configuration for descending simulations where the s-CNT is far away from the surface was first equilibrated in the *NPT* ensemble at 298 K using a velocity rescaling thermostat with a time constant of 0.5 ps and at 1 bar using a Berendsen barostat with a time constant of 2 ps. An anisotropic barostat was used to only adjust the size of the simulation box in the *z*-direction to achieve the correct solvent density while conserving the surface area of the SAM. Each configuration was further equilibrated in the

NVT ensemble for 4 ns. These equilibrated configurations were pulled towards the surface in the descending simulations. The configuration at the closest separation generated from the descending simulation was equilibrated for 2 ns with the s-CNT constrained to its initial positions, then this equilibrated configuration was used as the initial configuration for ascending simulations in which the s-CNT was pulled away from the surface. We thus obtained initial frames generated from ascending and descending simulations for each value of the reaction coordinate. Both initial frames were equilibrated for another 2 ns with the s-CNT constrained to its initial positions. Umbrella sampling was performed twice for each value of the reaction coordinate and all histograms were input to WHAM. Each umbrella sampling window was sampled for 20 ns, which is longer than the time for convergence based on prior estimates (~12 ns[1]). Error was estimated by bootstrapping.

S4. Surface Characterization from MD simulations

To characterize the SAM-grafted surfaces, we calculated the P_2 order parameter and tilt angle to quantify the orientational ordering of SAM molecules.

S4.1 P2 order parameter

The P_2 order parameter is usually used to describe the nematic ordering of liquid crystals. In this study, we use the P_2 order parameter to describe the orientational ordering of SAM molecules on the surface. The P_2 order parameter is defined as:

$$P2 = < \frac{3}{2} \cos^2 \theta - \frac{1}{2} >$$

where θ is the angle between the nematic director and molecular axis. The nematic director $\boldsymbol{n}_k$ is the eigenvector associated with the largest eigenvalue of the second rank ordering tensor $Q_k^{\alpha,\beta}$, which is given by

$$Q_k^{\alpha,\beta} = \frac{1}{N}\sum_{i=1}^{N}\left[\frac{3}{2}\boldsymbol{u}_k^{\alpha}\boldsymbol{u}_k^{\beta} - \frac{1}{2}\delta_{\alpha,\beta}\right]$$

where $\boldsymbol{u}_k$ is the long axis of a SAM molecule, N is the number of molecules, and $\delta_{\alpha,\beta}$ is the Kronecker delta function. The long axis of the molecule is found from the inertia tensor:

$$I_k^{\alpha,\beta} = \sum_{i=1}^{n} m_i\left[\boldsymbol{r}_i^2\delta_{\alpha,\beta} - \boldsymbol{r}_i^{\alpha}\boldsymbol{r}_i^{\beta}\right]$$

where $\boldsymbol{r}_i$ and m_i are the positions relative to the center of mass and masses of the atoms, respectively. n is the number of atoms in the molecule. The long axis $\boldsymbol{u}_k$ is the eigenvector associated with the smallest eigenvalue of $I_k^{\alpha,\beta}$. $P_2 = 0$ indicates a completely disordered phase and $P_2 = 1$ indicates a completely ordered phase.

S4.2 Tilt angle

The tilt angle is calculated as the average angle between (1) a vector from the silicon atom at the surface to the terminal carbon atom of a SAM molecule and (2) the vector normal to the surface.

S4.3 Relationship between structure parameters and s-CNT deposition

Figure S1 shows P_2 order parameters calculated for all simulated surfaces, with points colored based on whether s-CNT deposition is observed to be favorable. We find that there is no clear trend in these data – surfaces with both low values of P_2 (corresponding to disordered SAMs) and high values of P_2 (corresponding to ordered SAMs) exhibit favorable deposition, with a SAM for which deposition is not favorable based on PMF analysis (PEO) lying between these extremes. These data suggest that P_2 is a poor descriptor for deposition. Similarly, Figure S2 shows tilt angles computed for a subset of SAMs and again shows no clear correlation with deposition trends.

Together, these results indicate that parameters quantifying the structure of SAMs alone are poor descriptors of deposition, as might be expected given the lack of chemical features.

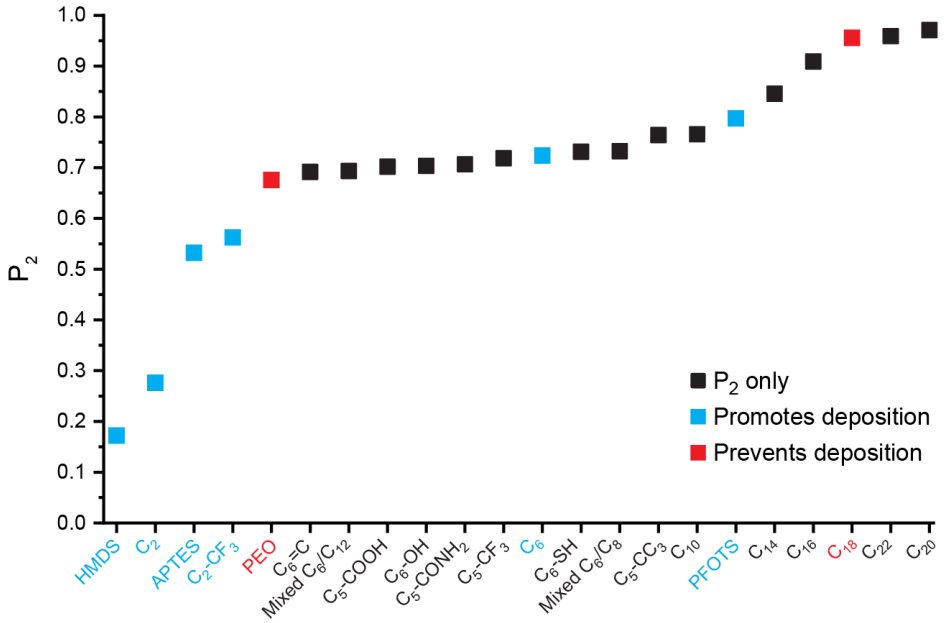

Figure S1. P2 order parameters for all surfaces considered in this study.

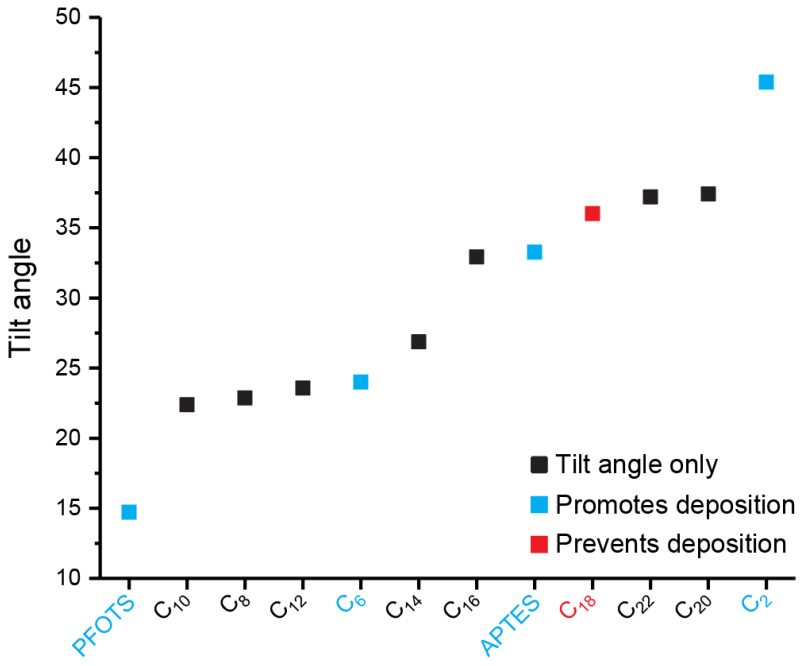

Figure S2. Tilt angle (°) of surfaces composed of alkyl chains as well as PFOTS and APTES.

S5. Solvent Structure near SAMs and the s-CNT

To understand the relationship between adsorption and solvent structure, we analyzed the relationship between solvent disruption and the potentials of mean force (PMF) computed in the main text. In bulk solution, a PFO-BPy-wrapped s-CNT also disrupts local solvent structure, leading to solvent density oscillations similar to those observed near the SAM-grafted surfaces that have high affinity for adsorption.[1] To test the hypothesis that favorable solvent-mediated forces emerge from the similar disruption of solvent when the s-CNT is adsorbed to a SAM-grafted surface, we computed the computed the locations of minima in the PMFs, the solvent density near the SAM-grafted surface, and the solvent structure relative to the center of mass (COM) of a s-CNT in bulk solution. We define $D_{\mathrm{min}}^{\mathrm{PMF}}$ as the location of the minimum in the PMF, $D_{\mathrm{min}}^{\mathrm{sol}}$ as the location of the minimum in the solvent density near each SAM-grafted surface (*e.g.*, the minimum value used to compute the peak:well ratio), and R as the location of the minimum in the solvent density near the s-CNT (computed as ~0.97 nm). We expect $D_{\mathrm{min}}^{\mathrm{PMF}}$ (corresponding to the COM distance for which adsorption is favorable) to equal the sum of $D_{\mathrm{min}}^{\mathrm{sol}}$ and R, which would indicate that this minima of the solvent density profiles near the SAM and the s-CNT coincide when adsorption is favorable. We thus define $\Delta = D_{\mathrm{min}}^{\mathrm{PMF}} - (D_{\mathrm{min}}^{\mathrm{sol}} + R)$ to measure the similarity between these metrics. Values of Δ for the C_2- and C_2-CF_3- grafted surfaces are less than 0.1 nm (Table S1). Somewhat larger Δ values (0.1-0.2 nm) are determined for the C_6- and PEO-grafted surfaces, but these surfaces are not expected to lead to strong adsorption so the discrepancy might arise from the uncertainties in determining the locations for the broad wells in PMFs of C_6 and PEO. The overall small Δ values indicate that $D_{\mathrm{min}}^{\mathrm{PMF}} \approx D_{\mathrm{min}}^{\mathrm{sol}} + R$ and supports the hypothesis that solvation forces which arise due to the layering of solvent molecules around s-CNTs in solution

and near SAM-grafted surfaces give rise to attractive interactions that thermodynamically favor deposition across a range of surfaces.

Table S1. Locations of PMF minima and solvent density minima as well as the relationships among them for C_2, C_6, C_2-CF_3, and PEO-grafted surfaces, respectively.

Surfaces	$D_{\min}^{\mathrm{PMF},1}$ (nm)	$D_{\min}^{sol,1} + R$ (nm)	Δ (nm)
C_2	2.77	2.82	0.05
C_6	3.85	3.67	-0.18
C_2-CF_3	3.32	3.32	0.00
PEO	4.1	3.93	-0.18

S6. Experimental Details for Silicon Substrate Functionalization

Silicon substrates were purchased from Addison Engineering, Inc. To clean the substrate prior to experiments, a silicon wafer approximately 1 × 1 cm^2 in size was immersed in a 3:1 by volume H_2SO_4/H_2O_2 piranha solution for 30 mins at 85 °C. After piranha treatment, substrates were rinsed with copious amounts of deionized (DI) water and dried with N_2. Substrates were functionalized immediately after piranha treatment with the desired SAM in a N_2 glove box. Trichloro(hexyl)silane and trichloro(3,3,3-trifluoropropyl)silane were purchased from Sigma-Aldrich. C_6-functionalized silicon substrates were fabricated by submerging the substrates in a trichloro(hexyl)silane solution with a concentration of 2.5 mM. After deposition for 12 h, substrates were sonicated in toluene for 30 min and dried with N_2 for surface characterization and CNT deposition. To functionalize the substrates with C2-CF_3, a solution with 0.25 vol% of trichloro(3,3,3-trifluoropropyl)silane in toluene was prepared and heated at 80 °C for 5 min.

Substrates were submerged in the solution for 10 min. The substrates were then sonicated in hexane for 10 min followed by annealing on a hot place at 150 °C for 1 h. The substrates were rinsed with hexane, dried and stored under vacuum. Water contact angle measurements were obtained using a Dataphysics OCA 15 optical contact angle system. Film thickness was measured by ellipsometry (Rudolph Research Auto EL) at three wavelengths (632.8 nm, 546.1 nm, 405 nm). Surface roughness and CNT densities on different SAMs were measured by AFM using a Bruker Multimode 8 AFM.

S7. Experimental Details for Preparation of s-CNT Inks

Inks of s-CNTs wrapped with PFO-BPy were prepared according to previously procedures.[1] In this process, arc-discharge nanotube soot (Sigma-Aldrich, #698695) was combined at a 1:1 ratio with PFO-BPy (American Dye Source, Inc., Quebec, Canada; #ADS153-UV) dispersed at 2 mg/mL in 60 mL of toluene. This mixture was sonicated at 40% amplitude with a horn tip sonicator (Thermo Fisher Scientific, Waltham, MA; Sonic Dismembrator 500) for 30 min. Undispersed nanotubes and other carbon allotropes were removed by centrifugation using a swing bucket rotor (Sorvall WX, TH-641, Thermo Fisher Scientific) at 3×10^5 *g* for 10 min. The upper 90% of the supernatant was collected, filtered, and then concentrated to ~ 60 mL using a rotary evaporator. This concentrated solution was centrifuged in a fixed rotor for 12 – 18 h to collect the PFO-BPy wrapped s-CNTs into pellets. These pellets were dispersed in toluene using the horn tip sonicator and again centrifuged for 12 – 18 h. This sonication/centrifugation process was repeated for a total of three times to remove excess PFO-BPy. The final s-CNT inks were prepared by dispersing the s-CNT pellets in either toluene or chloroform (stabilized with 0.75% ethanol, Thermo Fisher

Scientific, #C606-1) using tip sonication. Optical cross sections of the S_{22} transition were used to determine the s-CNT concentration in these inks.

SI References:

(1) Dwyer, J. H.; Shen, Z.; Jinkins, K. R.; Wei, W.; Arnold, M. S.; Van Lehn, R. C.; Gopalan, P. Solvent-Mediated Affinity of Polymer-Wrapped Single-Walled Carbon Nanotubes for Chemically Modified Surfaces. *Langmuir* **2019**, *35*, 12492–12500. https://doi.org/10.1021/acs.langmuir.9b02217.

(2) Emami, F. S.; Puddu, V.; Berry, R. J.; Varshney, V.; Patwardhan, S. V.; Perry, C. C.; Heinz, H. Force Field and a Surface Model Database for Silica to Simulate Interfacial Properties in Atomic Resolution. *Chem. Mater.* **2014**, *26* (8), 2647–2658. https://doi.org/10.1021/cm500365c.

(3) Mityashin, A.; Roscioni, O. M.; Muccioli, L.; Zannoni, C.; Geskin, V.; Cornil, J.; Janssen, D.; Steudel, S.; Genoe, J.; Heremans, P. Multiscale Modeling of the Electrostatic Impact of Self-Assembled Monolayers Used as Gate Dielectric Treatment in Organic Thin-Film Transistors. *ACS Appl. Mater. Interfaces* **2014**, *6* (17), 15372–15378. https://doi.org/10.1021/am503873f.

(4) Roscioni, O. M.; Muccioli, L.; Mityashin, A.; Cornil, J.; Zannoni, C. Structural Characterization of Alkylsilane and Fluoroalkylsilane Self-Assembled Monolayers on SiO 2 by Molecular Dynamics Simulations. *J. Phys. Chem. C* **2016**, *120* (27), 14652–14662. https://doi.org/10.1021/acs.jpcc.6b03226.

(5) Wang, J.; Wolf, R. M.; Caldwell, J. W.; Kollman, P. A.; Case, D. A. Development and Testing of a General Amber Force Field. *J. Comput. Chem.* **2004**, *25* (9), 1157–1174.

(6) Bayly, C. I.; Cieplak, P.; Cornell, W. D.; Kollman, P. A. ARTICLES A Well-Behaved Electrostatic Potential Based Method Using Charge Restraints for Deriving. *J. Phys. Chem.* **1993**, *97* (40), 10269–10280. https://doi.org/10.1021/j100142a004.

(7) D.A. Case, I.Y. Ben-Shalom, S.R. Brozell, D.S. Cerutti, T.E. Cheatham, III, V.W.D. Cruzeiro, T. A. D.; R.E. Duke, D. Ghoreishi, M.K. Gilson, H. Gohlke, A.W. Goetz, D. Greene, R Harris, N. Homeyer, Y. H.; S. Izadi, A. Kovalenko, T. Kurtzman, T.S. Lee, S. LeGrand, P. Li, C. Lin, J. Liu, T. Luchko, R. Luo, D. J.; Mermelstein, K.M. Merz, Y. Miao, G. Monard, C. Nguyen, H. Nguyen, I. Omelyan, A. Onufriev, F. Pan, R.; Qi, D.R. Roe, A. Roitberg, C. Sagui, S. Schott-Verdugo, J. Shen, C.L. Simmerling, J. Smith, R. S.-; Ferrer, J. Swails, R.C. Walker, J. Wang, H. Wei, R.M. Wolf, X. Wu, L. Xiao, D. M. Y. and P. A. K. AMBER 2018. University of California, San Francisco 2018.

(8) Pramanik, C.; Gissinger, J. R.; Kumar, S.; Heinz, H. Carbon Nanotube Dispersion in Solvents and Polymer Solutions: Mechanisms, Assembly, and Preferences. *ACS Nano* **2017**, *11* (12), 12805–12816. https://doi.org/10.1021/acsnano.7b07684.

(9) Kumar, S.; Bouzida, D.; Swedsen, R. H.; Kollman, P. A.; Rosenbergl, J. M. The Weighted Histogram Analysis Method for Free-Energy Calculations on Biomolecules. I. The Method. *J. Comput. Chem.* **1992**, *13* (8), 1011–1021.

(10) Jaster, A. The Hexatic Phase of the Two-Dimensional Hard Disk System. *Phys. Lett. Sect. A Gen. At. Solid State Phys.* **2004**, *330* (1–2), 120–125. https://doi.org/10.1016/j.physleta.2004.07.055.

(11) Dallin, B. C.; Van Lehn, R. C. Spatially Heterogeneous Water Properties at Disordered Surfaces Decrease the Hydrophobicity of Nonpolar Self-Assembled Monolayers. *J. Phys. Chem. Lett.* **2019**, *10* (14), 3991–3997. https://doi.org/10.1021/acs.jpclett.9b01707.